Design, optimization, and performance characterization of Terracotta Flat Tubular Direct Evaporative Cooler

ABSTRACT

This study presents the design and testing of a lab-scale Terracotta Flat Tubular direct evaporative cooler constructed from locally sourced materials. The key components of the system include a galvanized steel box, hollow baked clay tubes with a flat geometry, an axial fan, and a low-power submersible water pump. Experiments were conducted to evaluate the effects of varying intake air velocity, and water temperature.The experiment was carried out between2:30 PM and 5:00 PM where air temperature and humidity in the test room stabilize. The results demonstrated temperature reductions ranging from 5.9°C to 15.7°C, outlet relative humidity levels between 52% and 95%, and cooling effectiveness values from 0.41 to 1.11. The optimal performance of the cooler was achieved at air velocities of up to 1 m/s and water temperatures around 18°C, at which the Feasibility Index is less than 11 , which is in the range of the recommended value.The prototype achieved a cooling capacity of 62 W, with a coefficient of performance ranging from 3.3 to 5.6.Recommendations for future work include scaling up the system and enhancing its compactness to improve performance, making it suitable for enhancing indoor air quality and thermal comfort in rural households, schools, and offices with limited power access, as well as assisting small-scale farmers in reducing postharvest losses of horticultural products.

Keywords: Design; optimization; performance characterization, Terracotta Flat Tube, Direct Evaporative Cooler.

1. INTRODUCTION

In recent years, traditional air-conditioning systems, which rely on mechanical vapor compressors, have faced criticism for their high energy consumption[1] and use of synthetic refrigerants that contribute to global warming[2]. As a result, there is growing interest in developing low-energy alternatives[3], such as evaporative cooling, which provides thermal comfort with minimal power consumption and without harmful refrigerants[4]. Evaporative cooling, an environmentally friendly process that uses water as a working fluid, offers significant energy savings by reducing the reliance on mechanical compressors, with only pumps and fans as the primary energy-consuming components[5].There are two main types of evaporative cooling: direct and indirect. Direct evaporative cooling (DEC) cools and humidifies air by passing it over a wet surface, while indirect evaporative cooling (IEC) uses a heat exchanger to cool air without adding moisture[6]. Direct evaporative cooling (DEC) systems are highly efficient and easy to fabricate, particularly suited for hot and dry regions[7], [8]. Their global application has demonstrated significant energy savings and

simplicity in operation[9], [10]. The wet media used in DEC is crucial and typically made from porous materials with high water retention capacity[11]. Material selection depends on factors like application, effectiveness, cost, and environmental impact[12]. Research has explored various materials, such as hollow bricks, honeycomb paper, metals, fibers, ceramics, zeolite, and carbon, for their suitability in DEC[13]. Among these, porous ceramics stand out due to their corrosion resistance, availability, cost-effectiveness, and precise control over pore sizes[14]. Ceramics are versatile, durable, weather-resistant, and energy-efficient, making them ideal for building construction and various cooling applications, thereby contributing to energy efficiency and environmental sustainability construction[15], [16]. Their application in cooling systems, such as refrigeration and air conditioning, offers a sustainable and efficient solution for various cooling needs, contributing to energy efficiency and environmental sustainability. Among the various shapes of porous ceramic media, terracotta hollow tubes arranged to form a bundle also gain popularity as an evaporative cooling medium. Most of the research in terracotta tubular evaporative cooling focuses on cross-flow indirect and semi-indirect configurations[17], [18]. A semi-indirect made of terracotta hollow tubes was designed, manufactured, and tested byDubey et al.[19]. The proposed Semi Indirect Evaporative Cooler uses water-filled porous clay containers. Water seeps through the porous walls, wets the surface, and evaporates as air sweeps across, cooling both the surface and the air. Importantly, the cooled air does not carry water droplets. Only a small amount of water is added to the air, just enough to lower its temperature slightly. The air's temperature is further reduced through contact with the cooled pipe surface. Except for semi-indirect, the integration of terracotta tubes with heat pipes (HP) for indirect evaporative cooling systems has been extensively investigated. For instance, Alharbi et al.[20] demonstrated that a system with terracotta cuboids and finned heat pipes could cool air below its wet bulb temperature. For terracotta tubes used as cooling media, while circular shapes are standard for simplicity, specialized geometries like ovals enhance cooling capacity[21]. Despite the focus on semi-IECs and terracotta tubes integrated with heat pipes, there is a gap in research regarding the performance of a hollow terracotta tube with a compact flat geometry in direct evaporative cooling (DEC) applications.

In this study, a lab-scale Direct Evaporative Cooler made of terracotta hollow tubes was designed,manufactured, and tested under ambient air conditions.Terracotta, due to its porous structure, is well-suited to retain moisture and allow heat and mass exchange, thus creating an opportunity for use in evaporative cooling systems. The study includes fabricating the cooler's structure, manufacturing customized clay pipes, positioning them within the cooler, testing the system under laboratory conditions, and conducting a sensitivity analysis to determine optimal operating conditions.

2. MATERIAL AND METHODS

2.1. Cooler prototype and design consideration

The Terracotta Flat Tubular Direct Evaporative Cooler (TFT-DEC) was designed with economic and technical considerations to ensure feasibility and efficiency. The design aimed to minimize costs and maximize the reduction of supply air temperature. The cooler comprises a metal box crossed by porous baked clay tubes, with flat geometry to enhance compactness, wettability, and surface area. The system is sealed and insulated with a stainless galvanized steel box, a polystyrene layer, and an aluminum box. It includes two water tanks: a bottom tank for collecting water flowing down through the tubes, and a top tank with small holes for dispersing water through the tubes, supplied by a pump. Figure 1 shows the basic configuration of a TFT-DEC. As can be seen, porous ceramic is chosen as

the exchange medium to effectively hold water and ensure the wetting condition on its internal surface. In selecting construction materials, several factors were considered, including local availability, low cost, ease of handling during fabrication, material lightness, and environmental impacts such as non-toxicity and corrosion resistance.

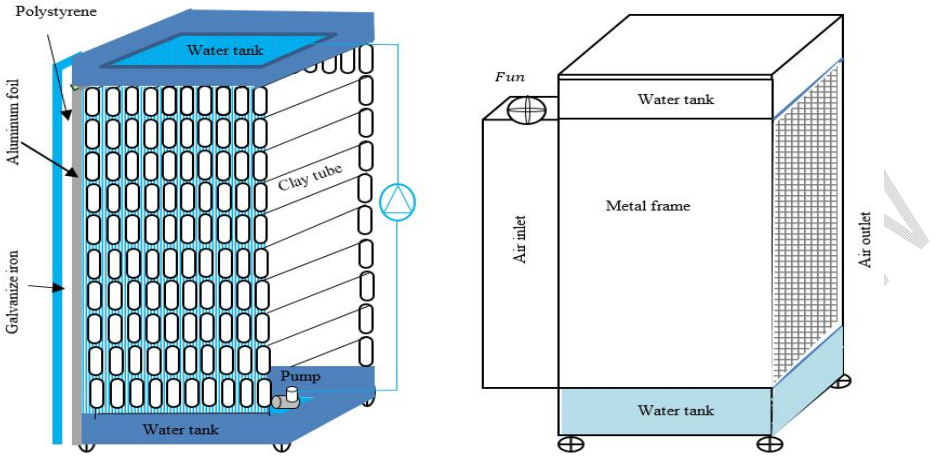

Figure 1: Prototype of the terracotta tube evaporative cooler

2.2. The operating principle of the cooler

The evaporative cooling system operates on the principle of water evaporation, where water absorbs heat from the air and evaporates, thereby lowering the air temperature. A water supply method was developed to continuously or intermittently spray water on the tube bundles using a water recirculation pump. Positioned atop the system is a water tank for collecting recirculated water used to irrigate the tube bundles. Additionally, at the lower section of the system, another water tank gathers falling water, which is then pumped back to the upper tank for recirculation. When the recirculation pump starts, a local wetting under the spraying region is formed. The wetting area gradually diffuses along the porous ceramic tubes by capillary action. After a sufficient spraying period, the outer surface of the tubes is completely wetted. The water stored in the upper part of the tubes reaches the limit, and then the excess water drips downward to the inner surface of the tubes to form the water film.The fan draws warm air from the outside environment and forces it through the wet tube channels. As the warm air passes through the tube channels, the film water covering the channel wall absorbs the heat from the air and evaporates. This process of evaporation removes heat from the air, resulting in a lower air temperature. The cooled air is then pushed by the fan into the interior spaces through ducts and vents, providing a cooling effect. The process continues as long as the system is operating, maintaining a continuous flow of cool air.

2.3. Construction materials

2.3.1. The cooling pad

The manufacturing process of terracotta tubes for use in this evaporative cooling system involves several key steps. Two types of clay, typically red and white, are carefully extracted from local deposits. The extracted clay is mixed in specific proportions to achieve the desired characteristics for the terracotta tubes. The clay is then crushed and kneaded to create a plasticine-like consistency. This paste is allowed to rest, enhancing its workability for

molding. The prepared clay paste is shaped into tubes using traditional hand-molding techniques. Once molded, the tubes are left to dry naturally at room temperature from a week. After drying, the tubes are placed in a kiln for firing. The kiln is gradually heated over a period of 30 hours, using sustainable fuels such as wood, and cow muck. Once the firing is complete, the kiln is allowed to cool for several days. After cooling, the terracotta tubes are carefully removed, sorted, and inspected for quality to ensure they meet the required standards. The finished terracotta tubes are shown in Figure 2. These tubes are designed to balance porosity for water flow and minimal wall thickness for heat exchange efficiency. The chemical compositions and the thermo physical properties of terracotta used in this work have been the subject of previous studies[22], [23].

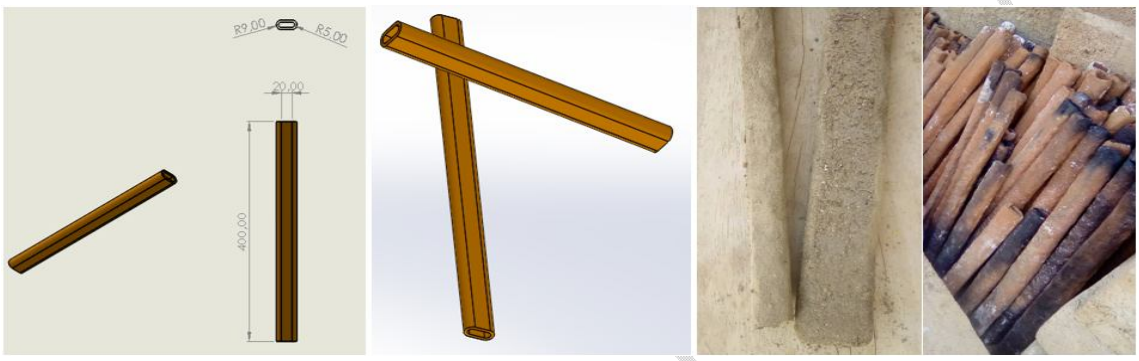

Figure 2: Cooling pad material

2.3.2. Other construction materials

The other materials used for the construction of this project are presented in Table 1

Table 1: Description of the construction materials

S/N	MATERIALS	QUANTITY	SPECIFICATIONS	NOTES
1	Galvanized steel	1	Thick: 0.8 mm Length: 1.5 m Width: 1 m	Used to make up the external wall of the cooling system.
2	Square pipe	4	1 by 1.2 m	Used for the framework of the entire cooler.
3	Aluminum sheet	1	Thick: 0.8 mm Length: 1.5 m Width: 1 m	It is used for the inner wall of the cooling system.

4	Water tank	2	10 liters	It is the water reservoir, both overhead and bottom tank.
5	Polystyrene	1	Thick: 2 cm Length: 1.5 m Width: 1 m	It is used as an insulating material to prevent the exchange of heat between the ambient and the cooler through its external and internal walls.
6	Suction fun	1	12 V DC 50/60 Hz 0.3 A	Used to blow ambient air through the wet clay tube.
7	Pump	1	8 W 10L/min	It makes the water circulate from the beneath reservoir to the overhead tank.
8	Connecting wire	2	2.5mm core 3 yards length	Used to connect the fans and the pump to electrical power
9	Tires	4	Diameter 3 cm	It enables effective mobility of the cooler
10	Paint	1/2	small blue box	For painting the exterior surface of the cooler.
11	Baked clay tubes	20	Length 400 mm Width 20 mm Internal radius 5 mm External radius 9 mm	Used as the cooling pad material

2.4. Fully assembly laboratory prototype

The assembly process of the cooler components is illustrated in Figure 3. Initially, wooden sheets were used to construct the cooler unit casing for accuracy verification (Figure 3a). The cooler features both internal and external caging systems (Figure 3b), with the outer casing made of galvanized steel measuring 45 cm in length, 35 cm in width, and 120 cm in height (Figure 3e). The fan and its housing are mounted on the rear side of the outer casing. The internal casing (Figure 3c), 120 cm high, 42 cm long, and 32 cm wide, is insulated with 2 cm thick polystyrene(Figure 3i) to prevent heat transfer. Inside, 20 porous ceramic tubes (Figure 3f) arranged in 4 horizontal and 5 vertical rows, encased within aluminum sheeting (Figure 3d), serve as the cooling pad. Two 10-liter water tanks, one below and one above the cooler, facilitate water recirculation using a 0.5 hp electric pump connected by a flexible plastic pipe. The water tanks and terracotta tubes are arranged from the base upwards, followed by the installation of the fan and the pump connected to a power supply. The fully assembled prototype, shown in Figure 3j, undergoes testing to ensure proper airflow, water distribution, and overall functionality.

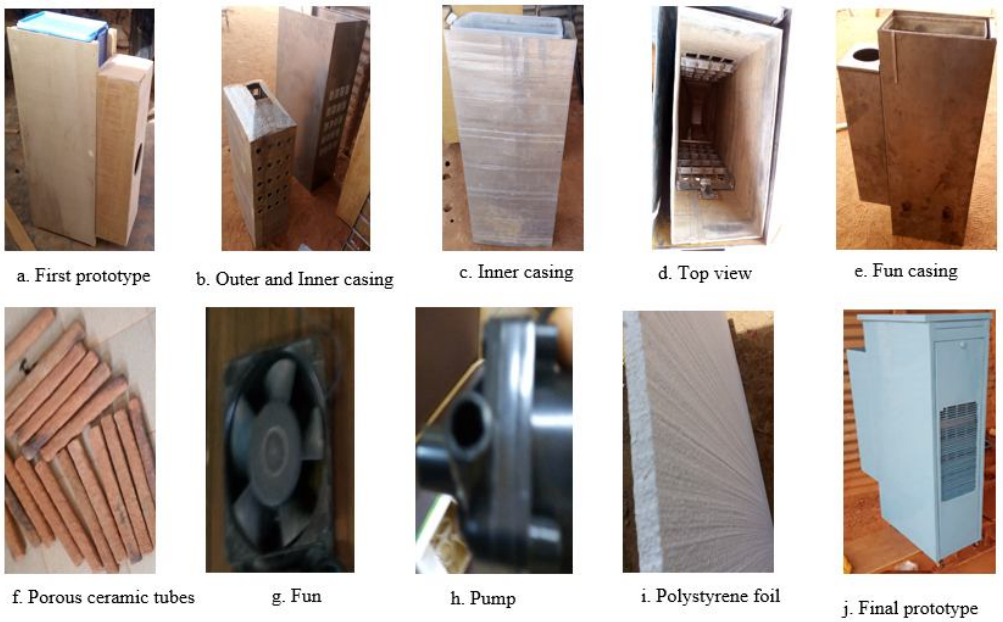

Figure 3: Prototype assembly components

2.5. Experimental setup and tests procedure

The fully assembled and insulated system, with all mechanical and electrical connections, is shown in Figure 4. The study took place in Ouagadougou, Burkina Faso, at coordinates -1.498928°E, 12.376962°N. Experimental tests were conducted to evaluate the performance of the developed cooler prototype and to examine the influence of air velocity, water temperature, and intermittent water supply schemes on the cooling performance. The experiments were conducted under uncontrolled indoor laboratory conditions during the hottest month of April. Due to the lack of an air-conditioning chamber, the temperature and humidity of the incoming air could not be controlled. Hence, a climate analysis of the test room was carried out prior to the tests to identify the period of the day during which indoor air conditions stabilized. Before each measurement, the cooling unit was run for more than one hour to wet the terracotta tubes completely. The steady-state conditions were achieved once the difference between the air's wet-bulb temperature, the tube wall temperature, and the water temperature stabilized. Measurements were taken at 2-minute intervals for each test except the dynamic operating performance test, for which measurements were taken every 10 minutes. A digital thermometer/hygrometer was used to measure air temperature and relative humidity at the inlet and outlet of the cooling unit. Water and tube wall temperatures were recorded using a digital reader connected to a type K thermocouple. An anemometer (UT363) was installed at the outlet to measure air velocity. The mass flow rate of air entering the cooling unit was determined using the air velocity and the total cross-sectional area of terracotta tubes. Airspeed was varied by adjusting the air intake section, and the water temperature was adjusted using chilled and hot water. A data logger (SM206-SOLAR) recorded data throughout the day to examine the cooler's dynamic operating performance. All these instruments were strategically placed around the test rig to collect the necessary data as presented in Figure 4. Table 2 summarizes the measured parameters and the corresponding instruments, including their ranges and accuracies.

Table 2: Test rig measurement materials

Parameter	Instrument/sensor	Range	Accuracy
Air velocity	Digital anemometer	0 to 10 m/s	±5 %
Air temperature	Thermometer/Hygrometer	-10 to +50 °C	±1°C
Air relative humidity	Thermometer/Hygrometer	10% - 99%	± 5%
Water temperature	Digital thermometer	-50 to +199.9 °C	±(0.3%+1°C)

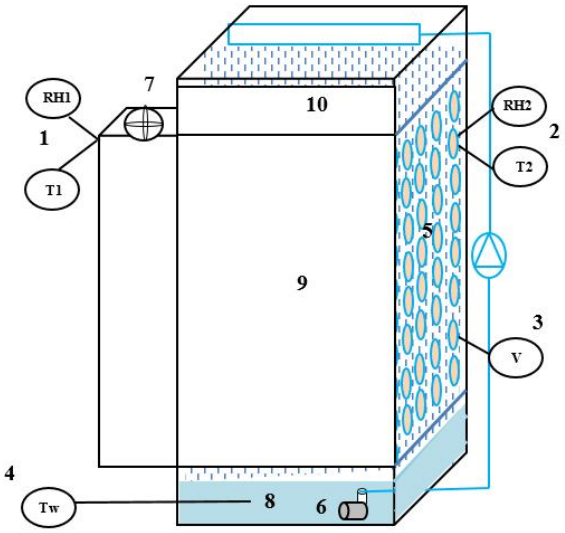

1&2 - Digital thermometer/hygrometer RH&T
3 – Digital anemometer
4 – Digital thermometer
5 – Wet terracotta tubes
6 – Water pump
7 – Fun at intake air section
8 – Water collector tank
9 – Metal box
10 – Water reservoir
11 – Data logger (SM206-SOLAR) for recording data.

Figure 4: Experimental setup

2.6. Performance evaluation

2.6.1. Temperature Drop (∆T):

The difference between the air inlet and outlet temperatures indicates the cooling effect of the unit.

$$\Delta T = T_{a,i} - T_{a,o} \quad (1)$$

Where $T_{a,i}$ is the inlet dry bulb temperature, $T_{a,o}$ is the outlet dry bulb temperature. The greater the difference between the two temperatures, the greater is the evaporative cooling effect [24].

2.6.2. Cooling Effectiveness (η_c):

Often expressed as a percentage, it measures how effectively the cooler lowers the air temperature compared to the maximum possible cooling (wet-bulb depression).

$$\eta_c = \frac{T_{a,i} - T_{a,o}}{T_{a,i} - T_{wb}} \quad (2)$$

Where T_{wb} is the inlet wet bulb temperature.

2.6.3 Airflow Rate (AFR):

The volume of air moved by the cooler is usually measured in cubic feet per minute (CFM) or cubic meters per hour (m^3/h).

$$AFR = 3600.N_t.\dot{V}_{a,o}.A_c \quad (3)$$

Where $\dot{V}_{a,o}$ is the supply air velocity, N_t is the number of tubes, and A_c represents tube's cross-section.

2.6.4. Cooling Capacity (CC)

The cooling capacity is the change in air sensible heat across the air channels of the DEC and is written as:

$$CC = \rho_{air}.AFR.C_{pa}\left(T_{a,i} - T_{a,o}\right) \quad (4)$$

Where ρ_{air} is the supply air density, and C_{pa} is the specific heat capacity at a constant pressure of the supply air ($J.kg^{-1}.K^{-1}$).

2.6.5. Coefficient Of Performance (COP)

The coefficient of performance is the ratio of the cooling capacity to the electrical power consumption of the fan and the pump. It is calculated by the following formula.

$$COP = \frac{CC}{P_{fan} + P_{pump}} = \frac{\rho_{air}.\dot{V}_{a,o}.C_{pa}\left(T_{a,i} - T_{a,o}\right)}{P_{fan} + P_{pump}} \quad (5)$$

Where P_{pump} is the power input to the water pump, and P_{fan} the power input to the fan.

2.6.6. Water evaporation rate (m_e)

The humidity of the dry air increases during its passage through the cooling pad due to the mass transfer of water vapor to the air. The following equation gives the amount of water evaporated (rate of water consumption).

$$m_e = \rho_a.AFR.\left(\omega_{a,o} - \omega_{a,i}\right) \quad (6)$$

Where $\omega_{a,i}$ and $\omega_{a,o}$ are the humidity ratios at the inlet and the outlet, respectively.

2.6.7. Faisibility Index (FI)

The Feasibility Index measures the disparity between inlet and outlet air temperatures. The small FI indicates better cooling performance in comparison with the higher value. This parameter is specified in Eq. (4). It evaluates the ability for evaporative cooling to provide human beings thermal comfort[25].

$$FI = T_{a,o} - \left(T_{a,i} - T_{a,o}\right) \quad (7)$$

The work of Camargo et al.[26] highlights the following ranges of the FI concerning cooling for human thermal comfort.

FI ≤ 10	Recommended for comfort cooling
11 ≤ FI ≤16	Recommended for relief (lenitive) cooling
FI > 16	Not recommended for the use of evaporative cooling systems

By evaluating these parameters, the performance of the evaporative cooler can be comprehensively assessed.

2.7. Experimental uncertainty

Uncertainty analysis evaluates the uncertainty of dependent variables. They are calculated analytically based on the error propagated while measuring the independent variables. Each experimental measurement has a certain degree of uncertainty and error due to instrument inaccuracy. In this study, errors during the measurement of airtemperatures, relative humidity, and air velocity were used to estimate the uncertainty of the performance parameterssuch as ΔT, η_c, CC, COP, and FIusing the formula given by equation(8)[27].

$$\Delta Y = \sqrt{\sum_{i=0}^{n} \left(\frac{\partial Y}{\partial X_i}\Delta X_i\right)^2} \quad (8)$$

Where Y is a given function of the independent variables X_1, X_2, X_3…. X_n which influence the dependent variable Y.

3. RESULTS AND DISCUSSION

3.1. Climatic study of the test room

This part of the study focuses on analyzing changes in air temperature and humidity within the test room to identify a period of stability for these parameters, which is essential for the accuracy and reliability of parametric tests. Figure 7 depicts the daily fluctuations in temperature and humidity over three consecutive days, revealing a clear pattern: temperature rises throughout the day, peaking around 3 PM, while humidity levels inversely decline, reaching their lowest point at the same time. It can be observed that air conditions stabilize between 2:30 PM and 5:00 PM, during which both temperature and humidity exhibit minimal fluctuations. Therefore, this period was chosen as the optimal time for conducting the parametric tests. This timeframe ensures stable air conditions, enhancing the accuracy and reproducibility of the findings.

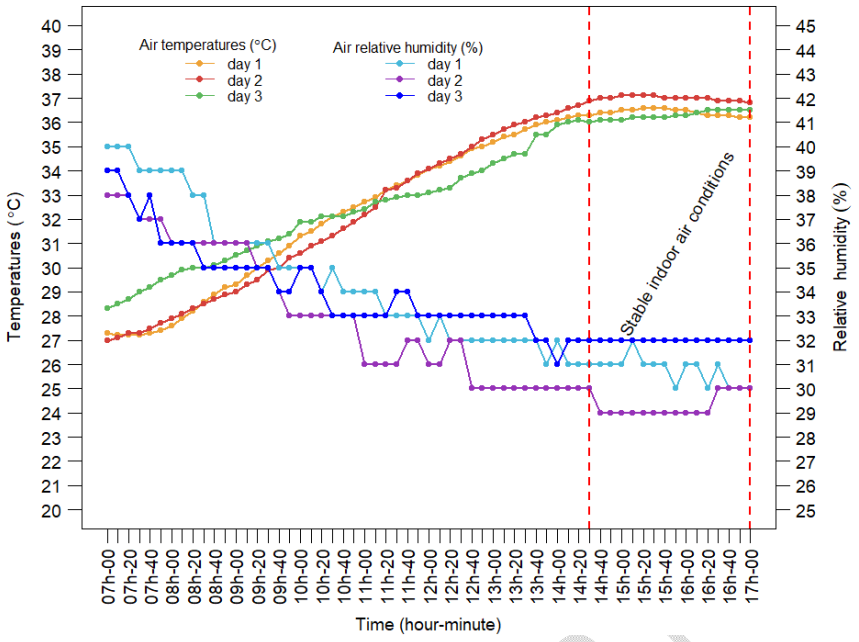

Figure 5: Daily fluctuations of air temperature and humidity in the test room over three consecutive days

3.2. Influence of intake air velocity on the outlet air temperature and humidity

Figure 6illustrates the outlet air temperature and humidity profiles at different intake air velocities. The results indicate that higher intake air velocities lead to increased outlet temperatures due to reduced residence time within the cooling system, which limits heat transfer between the air and the wet surface of the terracotta tube. Conversely, lower air velocities allow for longer contact time, enhancing heat transfer and resulting in lower outlet temperatures.However, if air velocity is too low, it can lead to quicker saturation, reducing the cooling potential as less sensible heat is available for conversion to latent heat through evaporation. Supporting findings from Al-Fahed et al.[28] and Fouda et al.[29]confirm that lower air velocities improve cooling effectiveness by facilitating better heat and mass transfer.The intake air velocity also affects the humidity of the outlet air. Higher velocities limit the absorption of water vapor, resulting in lower humidity, while lower velocities increase humidity levels due to extended contact with the evaporating water film. There is a trade-off between cooling effectiveness and humidity levels; high velocities may cool the air less effectively but maintain lower humidity, which can be beneficial in environments requiring controlled humidity. Conversely, lower velocities provide greater temperature drops but higher humidity, which may not be suitable in human comfort.Overall, the influence of intake air velocity on the terracotta tube evaporative cooling system must be balanced with considerations of system performance and energy efficiency. Higher velocities may increase energy consumption for air circulation, while excessively low velocities could hinder achieving desired cooling capacities.

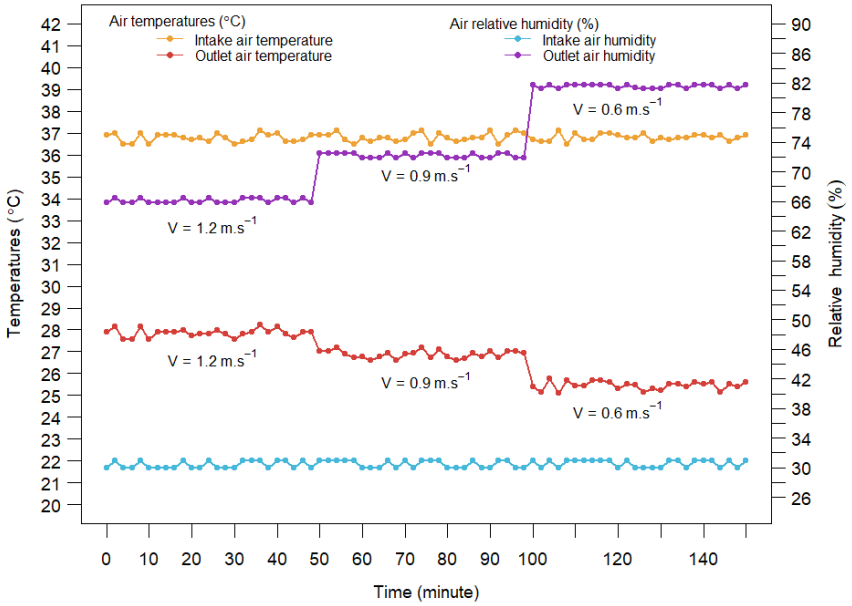

Figure 6: Influence of intake air velocity on the outlet air temperature and humidity

3.3. Influence of water temperature on the outlet air temperature and humidity

This experiment investigates the impact of varying water temperatures on the outlet air temperature and humidity in a Terracotta Flat Tubular Direct Evaporative Cooling System (TFT-DEC). The results, as illustrated in Figure 3 indicate that lower water temperatures significantly enhance the cooling effect, resulting in reduced outlet air temperatures and humidity. Cooler water temperatures reduce both the intake air's dry and wet-bulb temperatures, enabling the cooler to effectively cool and dehumidify the incoming air through condensation, provided the water temperature is below the air dew point temperature. Higher water temperatures, however, increase latent heat transfer, leading to higher air moisture content and humidity, and a reduced temperature drop. Previous studies support these findings. Sheng et al.[30] found that lower water temperatures improved saturation effectiveness but noted that cooling water below a certain threshold had minimal additional impact. Nada et al.[31] observed similar effects with varying water temperatures, and Al-Badri et al. [32] reported performance improvements with chilled water temperatures between the wet bulb temperature (WBT) and dew point temperature (DPT) of the inlet air. At each change of air velocity, we note that the system takes 8 to 10 minutes to reach a new steady state condition. This shows clearly that the thermal mass of the terracotta affects the outlet air temperature and humidity response. Overall, this study highlights the critical role of water temperature in the performance of terracotta evaporative cooling systems and suggests that adjusting water temperature can enhance system efficiency across different climate conditions.

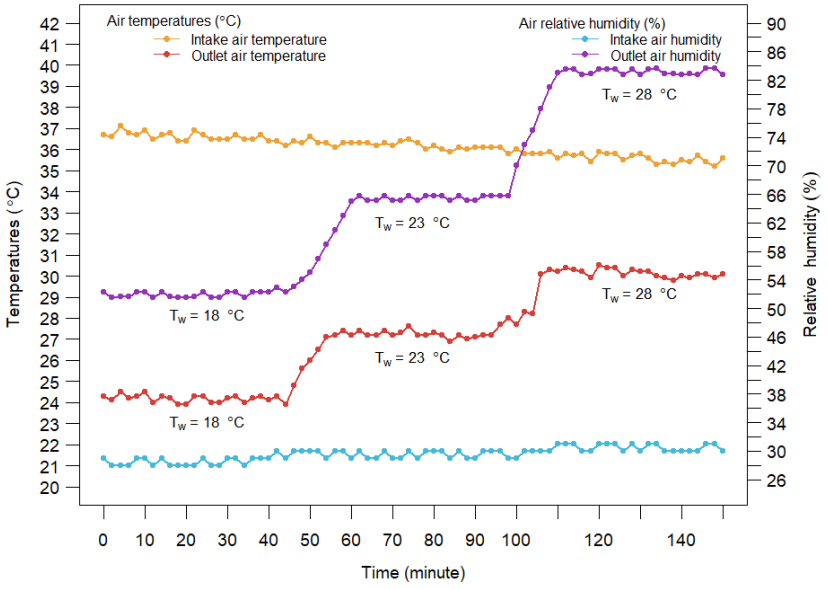

Figure 7: Influence of water temperature on the outlet air temperature and humidity

3.4. The dynamic operating performance of the cooler

This experiment consists of dynamic testing of the cooler to investigate the thermal performance under real operating conditions for a day-long period, and to examine its ability to meet the thermal comfort requirement. For hot and dry climate regions, typical indoor comfort is around 25 ℃ and 50-60% relative humidity, according to ASHRAE 55[33, p. 55]. The test was performed under ambient air conditions by setting the fun velocity and the initial temperature of the supply water at 1 m/s and 18 ^{o}C respectively. The recorded air temperature and humidity at the inlet and outlet of the cooler as well as the supply water temperature, are presented in Fig. 6. From the graph, the ambient air temperatures ranged from 28-37℃ with humidity of 30-39%, respectively. The maximum temperature reduction of 12℃ occurred at an ambient temperature of 37℃ and humidity of 30%, while the minimum reduction of 10℃ was observed at 28℃ and humidity of 37%. This indicates that the cooler's performance improves as the ambient temperature rises and humidity decreases. This advantage sets evaporative coolers apart from vapor-compressed cooling systems, whose performance typically decreases with increasing ambient temperatures[34]. Furthermore, it can be seen that in such climate conditions, the cooler demonstrated the ability to supply air at temperatures ranging from 18-25℃ with humidity ranging from 54-58%, which is in the comfort zone. This indicates that the developed cooler has the potential to meet the thermal comfort requirements in hot and dry climate regions, contributing to improved living conditions in such environments.

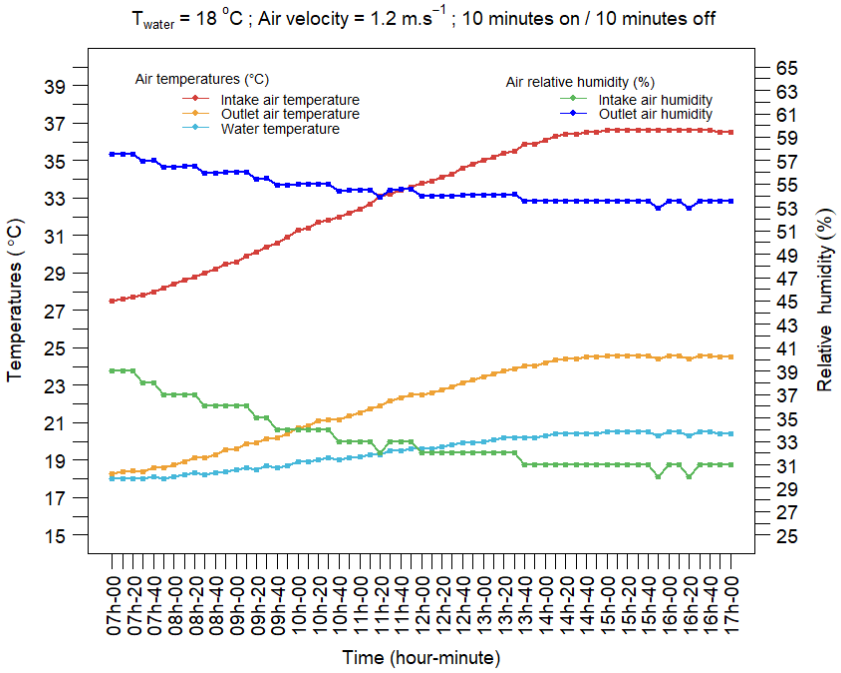

Figure 9: The dynamic operating performance of the cooler

3.5. Performance characterization of the cooler

Table 3 provides a quick overview of the cooler's performance parameters based on the experimental investigations under ambient air temperature of 36.5°C with 29% relative humidity. The performance of the cooler is measured in terms of supply air temperature and humidity, cooling capacity, coefficient of performance (COP), wet bulb effectiveness as well as cooler power and water consumption. The total wet surface area of the cooler prototype is estimated at 0.45 m^2. Comparison among the test results under the various operating conditions indicates that the optimum performance of the cooler is obtained at the lower recirculating water temperature (18 ^oC) and moderated air velocity (1.2 m/s), at which it delivers a cooling capacity of 62 W, equivalent to a specific cooling capacity of 136 W/m² of wet surface area. Under the same optimum conditions, the cooler dropped the ambient air temperature (36.5°C, 29% RH) by 12.7°C, achieving a wet bulb effectiveness of 0.87 and a COP of 3.3. However, adjustments to the air velocity affect the cooler's performance. Decreasing the air velocity beyond 1.2 m/s enhances the temperature drop and the wet bulb effectiveness but compromises the cooling capacity and COP due to reduced airflow rate. Higher recirculating water temperatures (above 23°C) also degrade the system's performance, leading to higher humidity levels and potentially greater discomfort. Thus, it's advisable to keep the recirculating water temperature close to or below the wet bulb temperature of the working air. Regarding water efficiency, the cooler operates efficiently at the optimum conditions, consuming between 0.010 and 0.015 liters per hour, equating to 0.167-0.25 liters per kilowatt-hour of cooling. This level of water usage marks a substantial improvement over cellulose pads evaporative cooling systems[35]. Also, it can be seen that the efficiency of the cooler can be greater than 1. This happens when the temperature of the water film at the tube-air interface is lower than the inlet air's wet bulb temperature. The lower water temperatures decrease both the intake air dry and wet-bulb temperatures,

causing the process to deviate from adiabatic saturation. In that condition, the cooler can cool and dehumidify the entering air by condensation if the water temperature is lower than the air dew point temperature. Although the system's COP is good compared with conventional air conditioners, this performance is still low compared with most recently developed DEC systems[8], [31]. Nevertheless, this performance can be considerably improved by increasing the size of the system, as well as its compactness. Also, the use of a special water reservoir of sufficient capacity with nozzles, combined with an intermittent pumping system, can significantly reduce pump consumption, thereby improving the system's COP.

Table 3: Performance characterization of the cooler at $T_{a,i}$ = 36.5 and $\emptyset_{a,i}$ = 29 %

Parameters	**Value**			**Value**			**Value**			**Error**
Water temperatures (^{o}C)	18			23			28			±1°C
Inlet air velocities (m.s^{-1})	1.2	0.9	0.6	1.2	0.9	0.6	1.2	0.9	0.6	±5 %
Inlet air flow rate (m^{3}/h)	15.3	11.4	7.6	15.3	11.4	7.6	15.3	11.4	7.6	±0.06
Supply air temp. (^{o}C)	24.2	22.7	20.8	27.4	26.3	24.9	31	30	29.0	±1 %
Feasibility index (FI)	11.9	8.9	5,1	18.3	16,1	13.3	25.5	23.5	21.5	±1.7
Supply air RH (%)	52	56	62	65	71	81	82	91	95	±5 %
Temperature drop (^{o}C)	12.3	13.8	15.7	9.1	10.2	11.6	5.9	6.5	7.5	±1.4°C
Wet-bulb efficiency (%)	0.87	0.97	1.11	0.64	0.72	0.82	0.41	0.46	0.53	±0.01
Cooling capacity (W)	62	53	41	46	38	29	29	24	19	±3.6
Power (W) Pump on	19	19	19	19	19	19	19	19	19	
COP Pump on	3.3	2.9	2.1	2.4	2	1.5	1.5	1.3	1	±0.3
Water consumption (l/h)	0.015	0.013	0.010	0.069	0.058	0.044	0.137	0.115	0.088	±0.007

4. CONCLUSION

This study successfully designed and tested a lab-scale Terracotta Flat Tubular Direct Evaporative Cooler (TFT-DEC) using locally sourced materials, demonstrating its potential as an efficient and sustainable cooling solution. The experimental results showed significant temperature reductions (5.9°C to 15.7°C) and relative humidity levels (52% to 95%), with cooling effectiveness values ranging from 0.41 to 1.11. Optimal performance was achieved at an intake air velocity of up to 1 m/s and a water temperature of approximately 18°C. An intermittent water supply cycle of 15 minutes on and 15 minutes off was found to balance water usage and energy efficiency effectively, maintaining cooling performance.The cooler's feasibility was confirmed by its coefficient of performance (3.3 to 5.6) and cooling capacity of 62 W, making it suitable for applications in rural households, schools, offices, and small-scale livestock settings. Future research should focus on scaling up the system and

enhancing its compactness to improve performance and expand its applicability in diverse settings.

REFERENCES

[1] S. S. Chandel, A. Sharma, and B. M. Marwaha, “Review of energy efficiency initiatives and regulations for residential buildings in India,” *Renew. Sustain. Energy Rev.*, vol. 54, pp. 1443–1458, Feb. 2016, doi: 10.1016/j.rser.2015.10.060.

[2] L. Yang, H. Yan, and J. C. Lam, “Thermal comfort and building energy consumption implications–a review,” *Appl. Energy*, vol. 115, pp. 164–173, 2014.

[3] B. Givoni, “Performance and applicability of passive and low-energy cooling systems,” *Energy Build.*, vol. 17, no. 3, pp. 177–199, 1991.

[4] S. Delfani, J. Esmaeelian, H. Pasdarshahri, and M. Karami, “Energy saving potential of an indirect evaporative cooler as a pre-cooling unit for mechanical cooling systems in Iran,” *Energy Build.*, vol. 42, no. 11, pp. 2169–2176, 2010.

[5] S. Li and J.-W. Jeong, “Energy performance of liquid desiccant and evaporative cooling-assisted 100% outdoor air systems under various climatic conditions,” *Energies*, vol. 11, no. 6, p. 1377, 2018.

[6] O. Amer, R. Boukhanouf, and H. G. Ibrahim, “A review of evaporative cooling technologies,” *Int. J. Environ. Sci. Dev.*, vol. 6, no. 2, p. 111, 2015.

[7] J. R. Camargo, C. D. Ebinuma, and J. L. Silveira, “Experimental performance of a direct evaporative cooler operating during summer in a Brazilian city,” *Int. J. Refrig.*, vol. 28, no. 7, pp. 1124–1132, 2005.

[8] K. Sellami, M. Feddaoui, N. Labsi, M. Najim, M. Oubella, and Y. K. Benkahla, “Direct evaporative cooling performance of ambient air using a ceramic wet porous layer,” *Chem. Eng. Res. Des.*, vol. 142, pp. 225–236, Feb. 2019, doi: 10.1016/j.cherd.2018.12.009.

[9] E. A. Awafo, S. Nketsiah, M. Alhassan, and E. Appiah-Kubi, “Design, Construction, and Performance Evaluation of an Evaporative Cooling System for Tomatoes Storage,” *Agric. Eng.*, vol. 24, no. 4, pp. 1–12, Dec. 2020, doi: 10.1515/agriceng-2020-0031.

[10] A. Laknizi, A. Ben Abdellah, M. Faqir, E. Essadiqi, and S. Dhimdi, “Performance characterization of a direct evaporative cooling pad based on pottery material,” *Int. J. Sustain. Eng.*, vol. 14, no. 1, pp. 46–56, Jan. 2021, doi: 10.1080/19397038.2019.1677800.

[11] T. Gunhan, V. Demir, and A. K. Yagcioglu, “Evaluation of the Suitability of Some Local Materials as Cooling Pads,” *Biosyst. Eng.*, vol. 96, no. 3, pp. 369–377, Mar. 2007, doi: 10.1016/j.biosystemseng.2006.12.001.

[12] S. Wanphen and K. Nagano, “Experimental study of the performance of porous materials to moderate the roof surface temperature by its evaporative cooling effect,” *Build. Environ.*, vol. 44, no. 2, pp. 338–351, 2009.

[13] X. Zhao, S. Liu, and S. B. Riffat, “Comparative study of heat and mass exchanging materials for indirect evaporative cooling systems,” *Build. Environ.*, vol. 43, no. 11, pp. 1902–1911, 2008.

[14] J. He and A. Hoyano, “Experimental study of cooling effects of a passive evaporative cooling wall constructed of porous ceramics with high water soaking-up ability,” *Build. Environ.*, vol. 45, no. 2, pp. 461–472, 2010.

[15] E. Ibrahim, L. Shao, and S. B. Riffat, “Performance of porous ceramic evaporators for building cooling application,” *Energy Build.*, vol. 35, no. 9, pp. 941–949, Oct. 2003, doi: 10.1016/S0378-7788(03)00019-7.

[16] W. Chen, S. Liu, and J. Lin, “Analysis on the passive evaporative cooling wall constructed of porous ceramic pipes with water sucking ability,” *Energy Build.*, vol. 86, pp. 541–549, 2015.
[17] E. Gomes, F. R. Martinez, F. V. Diez, M. M. Leyva, and R. H. Martin, “Description and Experimental results of a semi-indirect ceramic evaporative cooler. Int,” *J. Refrig.*, vol. 28, pp. 654–662, 2005.
[18] R. H. Martín, “Characterization of a semi-indirect evaporative cooler,” *Appl. Therm. Eng.*, vol. 29, no. 10, pp. 2113–2117, 2009.
[19] M. Dubey and S. Rajpat, “Development and performance evaluation of a semi indirect evaporative cooler,” 2008.
[20] A. Alharbi, A. Almaneea, and R. Boukhanouf, “Integrated hollow porous ceramic cuboids-finned heat pipes evaporative cooling system: Numerical modelling and experimental validation,” *Energy Build.*, vol. 196, pp. 61–70, 2019.
[21] A. Hasan and K. Sirén, “Performance investigation of plain circular and oval tube evaporatively cooled heat exchangers,” *Appl. Therm. Eng.*, vol. 24, no. 5–6, pp. 777–790, Apr. 2004, doi: 10.1016/j.applthermaleng.2003.10.022.
[22] S. Kam *et al.*, “Permeability to water of sintered clay ceramics,” *Appl. Clay Sci. - APPL CLAY SCI*, vol. 46, pp. 351–357, Dec. 2009, doi: 10.1016/j.clay.2009.09.005.
[23] S. Kam, M. Zongo, B. Dianda, A. Konfe, D. Bathiebo, and L. Aurelien, “Study of hygrothermal transfer through porous clay tubes application to the cooling of water volume in the sahelian zone,” *Adv. Appl. Sci. Res.*, vol. 3, no. 4, pp. 2090–2102, 2012.
[24] G. Chiesa, N. Huberman, and D. Pearlmutter, “Geo-climatic potential of direct evaporative cooling in the Mediterranean Region: A comparison of key performance indicators,” *Build. Environ.*, vol. 151, pp. 318–337, 2019.
[25] John R. Watt & Brown K.B., *Evaporative Air Conditioning Handbook*, Third ed. UK: Chapmann and Hall, 1997.
[26] J. Camrago, C. D. Ebinuma, and S. Cardoso, “Three methods to evaluate the use of evaporative cooling for human thermal comfort,” *Therm. Eng.*, vol. 5, no. 02, pp. 09–15, 2006.
[27] R. J. Moffat, “Describing the uncertainties in experimental results,” *Exp. Therm. Fluid Sci.*, vol. 1, no. 1, pp. 3–17, 1988.
[28] S. Al-Fahed, F. Alasfour, and M. Quadri, “Pottery evaporative cooling system: a novel approach to cool inlet air with minimal change in relative humidity and low water consumption,” *Exp. Heat Transf.*, vol. 27, no. 2, pp. 144–159, 2014.
[29] A. Fouda and Z. Melikyan, “A simplified model for analysis of heat and mass transfer in a direct evaporative cooler,” *Appl. Therm. Eng.*, vol. 31, no. 5, pp. 932–936, 2011.
[30] C. Sheng and A. A. Nnanna, “Empirical correlation of cooling efficiency and transport phenomena of direct evaporative cooler,” presented at the ASME International Mechanical Engineering Congress and Exposition, 2011, pp. 953–967.
[31] S. A. Nada, H. F. Elattar, M. A. Mahmoud, and A. Fouda, “Performance enhancement and heat and mass transfer characteristics of direct evaporative building free cooling using corrugated cellulose papers,” *Energy*, vol. 211, p. 118678, Nov. 2020, doi: 10.1016/j.energy.2020.118678.
[32] A. R. Al-Badri and A. A. Al-Waaly, “The influence of chilled water on the performance of direct evaporative cooling,” *Energy Build.*, vol. 155, pp. 143–150, 2017.
[33] P. ASHRAE, “Heating and cooling, ASHRAE Handbook-HVAC Systems and Equipment, SI ed,” *Am. Soc. Heat. Refrig. Air-Cond. Eng. ASHRAE Atlanta GA US*, 2008.
[34] I. M. Baca, S. M. Tur, J. N. Gonzalez, and C. A. Román, “Evaporative cooling efficiency according to climate conditions,” *Procedia Eng.*, vol. 21, pp. 283–290, 2011.
[35] A. Malli, H. R. Seyf, M. Layeghi, S. Sharifian, and H. Behravesh, “Investigating the performance of cellulosic evaporative cooling pads,” *Energy Convers. Manag.*, vol. 52, no. 7, pp. 2598–2603, 2011.